NANO LETTERS

Letter

pubs.acs.org/NanoLett

# Active Tunable Absorption Enhancement with Graphene Nanodisk Arrays

Zheyu Fang,*[,†,#,‡] Yumin Wang,[‡] Andrea E. Schlather,[▽] Zheng Liu,[□] Pulickel M. Ajayan,[⊥] F. Javier García de Abajo,[§,∥] Peter Nordlander,[†,‡,○] Xing Zhu,[†] and Naomi J. Halas*[,‡,▽,○]

[†]School of Physics, State Key Lab for Mesoscopic Physics, Peking University, Beijing 100871, China

[#]Collaborative Innovation Center of Quantum Matter, Beijing 100871, China

[‡]Department of Electrical and Computer Engineering, and the Laboratory for Nanophotonics, Rice University, 6100 Main Street, Houston, Texas 77005, United States

[▽]Department of Chemistry, Rice University, 6100 Main Street, Houston, Texas 77005, United States

[□]School of Materials Science and Engineering, School of Electrical and Electronic Engineering, Nanyang Technological University, 50 Nanyang Ave., Singapore 639798

[§]ICFO—Institut de Ciencies Fotoniques, Mediterranean Technology Park, 08860 Castelldefels, Barcelona, Spain

[∥]ICREA—Institució Catalana de Reserca i Estudis Avançats, Passeig Lluís Companys, 23, 08010 Barcelona, Spain

[⊥]Mechanical Engineering and Materials Science Department, Rice University, Houston, Texas 77005, United States

[○]Department of Physics and Astronomy, Rice University, Houston, Texas 77005, United States

**ABSTRACT:** If not for its inherently weak optical absorption at visible and infrared wavelengths, graphene would show exceptional promise for optoelectronic applications. Here we show that by nanopatterning a graphene layer into an array of closely packed graphene nanodisks, its absorption efficiency can be increased from less than 3% to 30% in the infrared region of the spectrum. We examine the dependence of the enhanced absorption on nanodisk size and interparticle spacing. By incorporating graphene nanodisk arrays into an active device, we demonstrate that this enhanced absorption efficiency is voltage-tunable, indicating strong potential for nanopatterned graphene as an active medium for infrared electro-optic devices.

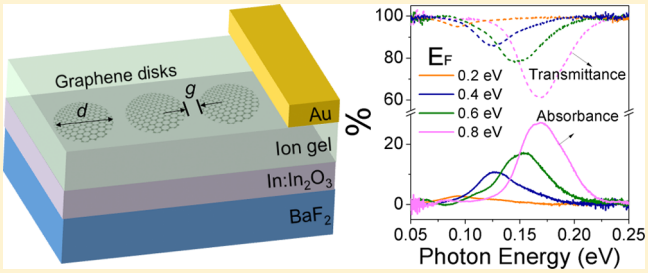


**KEYWORDS:** *Surface plasmon, graphene, antenna, optical absorber, optical tunability*

Graphene, consisting of a single layer of carbon atoms in a honeycomb lattice, has been recognized as a promising two-dimensional material for a wide range of applications such as transparent electronics, gate modulators, photocatalysts, and more.[1−10] However, because of its single-atom-layer thickness and low photoconductivity in the visible region of the spectrum, graphene interacts with light very inefficiently. A single sheet of homogeneous graphene absorbs only 2.3% of normal incidence light in the visible and near-infrared range,[11] while an absorption of 10% can be achieved with evanescent excitation when the graphene layer is incorporated into a multilayer dielectric structure.[12] Gold plasmonic nanoantennas fabricated onto graphene have also been shown to substantially enhance its light-harvesting efficiency.[13−17]

An alternative approach for enhancing optical absorption in graphene is to exploit the comparatively stronger absorption properties of the localized plasmon resonances of graphene nanostructures.[18−20] Because direct optical excitation and facile electrical tunability of the plasmons of graphene nanostructures are both possible, this approach shows excellent potential for device applications. The use of subwavelength structures enables one to overcome the momentum and energy mismatch between photons and plasmons characteristic of optical excitation of surface plasmons on extended films. Nanopatterning of graphene can be achieved using e-beam lithography and subsequent lift-off to produce structures such as nanodisks, nanorings, and nanoribbons, all of them capable of supporting localized and propagating plasmons.[21,22] Because graphene is significantly less lossy than traditional plasmonic materials (e.g., coinage metals),[23] its plasmons can exhibit large *Q*-factors, resulting in narrow absorption profiles. By stacking graphene/insulator disks, the device absorption can be further increased.[24] Since the Fermi level of graphene is readily controlled by applying a voltage (electrostatic doping),[25−27] a wide range of plasmon tunability in the IR is possible in device geometries.[21,22]

**Received:** October 30, 2013
**Revised:** December 2, 2013
**Published:** December 9, 2013

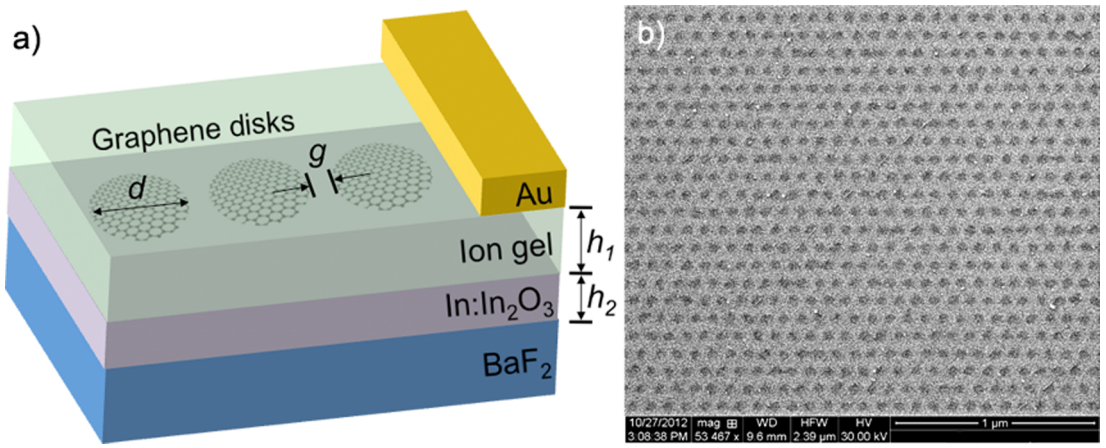


**Figure 1.** (a) Scheme of the measured devices. A graphene monolayer was transferred to a In−$In_2O_3$/$BaF_2$ substrate and subsequently patterned with e-beam lithography. The ion-gel was spin-coated on top of the graphene nanostructure, and the Au gate contact deposited on the top. The thickness of the ion-gel layer was $h_1$ = 100 nm and the thickness of In−$In_2O_3$ layer $h_2$ = 20 nm. (b) SEM image showing a fabricated array on Si/$SiO_2$ of closely packed graphene nanodisks with diameter $d$ = 60 nm and an edge-to-edge disk gap of ∼30 nm.

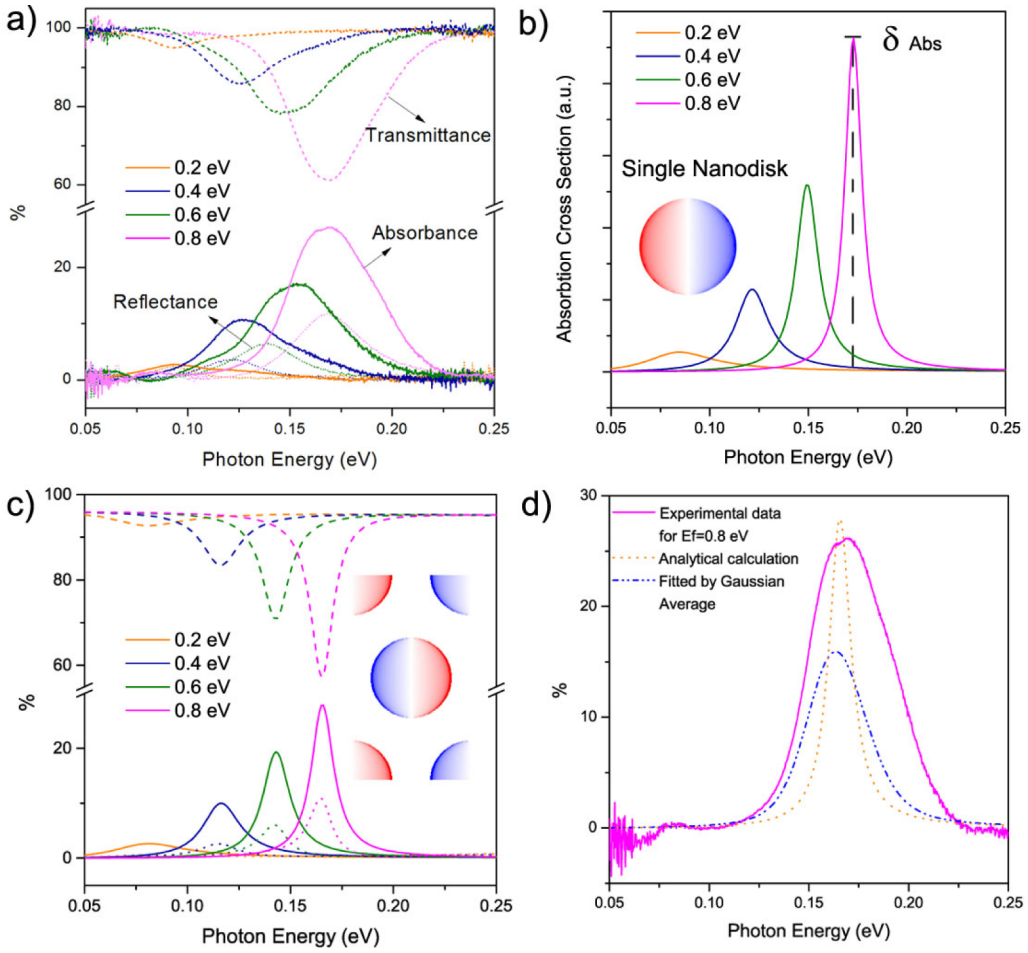


**Figure 2.** (a) FTIR measurements of transmittance, reflectance, and absorbance for graphene nanodisk arrays with the Fermi energy ranging from 0.2 to 0.8 eV. (b) Calculated individual graphene nanodisk absorption cross-section for the same range of Fermi energies. The inset shows the plasmon induced charge density for a single nanodisk. (c) Analytical calculations for the nanostructures in panel a. (d) Effect of nonuniform lattice spacing obtained using a Gaussian average of the simulated absorption for arrays with different lattice constants consistent with the SEM images (blue) compared with both experimental data (purple) and the simulation for the nominal lattice constant (dashed yellow curve).

It has recently been theoretically predicted that complete optical absorption should be possible in closely packed graphene disk arrays positioned above a metallic plane when the cross section of each individual graphene disk is comparable to the area of the lattice unit cell.[28] In this Letter, we demonstrate significantly enhanced graphene absorption (30%) in arrays of graphene nanodisks, without the underlying metallic layer. In these arrays, the extinction cross-section of


dx.doi.org/10.1021/nl404042h | Nano Lett. 2014, 14, 299−304

each disk is designed to be comparable to the area of the unit cell, so that the enhanced absorption effect is maximized and a significant fraction of the incident light is absorbed, exciting graphene plasmons. A high-capacitance ion-gel layer was used to raise the Fermi level of narrow graphene nanodisks to 0.8 eV above the Dirac point, contributing to absorption enhancement as well as plasmon tuning.[22] In addition to a modulation of the plasmon frequency $\omega_p \sim (E_F/D)^{1/2}$ obtained by tuning the Fermi energy $E_F$ and the nanodisk diameter ($D$), we establish that absorption enhancement also depends on these same parameters. In addition, the optical absorption is strongly modulated by varying the distance between adjacent nanodisks.

A continuous, uniform atomic monolayer of graphene was grown by an optimized chemical vapor deposition method using $CH_4$ as the carbon source and $Ar/H_2$ as carrier gas. The as-grown graphene was first transferred onto a $BaF_2$ substrate coated with a thin layer of In−$In_2O_3$− via atomic layer deposition (ALD), then patterned into closely packed nanodisk arrays using e-beam lithography with poly(methyl methacrylate) (PMMA) as an electron beam resist. Oxygen plasma (40 W, 500 mT, 15 s) was used to etch away the exposed area, leaving the periodic pattern of graphene nanodisks protected by a PMMA layer, which was then removed with acetone. A schematic of the measurement configuration is shown in Figure 1a. Figure 1b shows a scanning electron microscopy (SEM) image of a graphene nanodisk array on a $Si/SiO_2$ substrate with disk diameters of 60 nm and a 30 nm interdisk gap distance. To tune the Fermi level of the graphene nanostructure array, a high capacitance ion-gel layer (the physically cross-linked, ionic liquid/triblock copolymer gel, see below) was spin-coated on top of the layer of graphene nanostructures. The Au electrodes used as top gates for the electrostatic doping were directly deposited onto the ion-gel layer, while the In−$In_2O_3$ film served as the bottom gate of the device.

The In−$In_2O_3$ film is used as a conductive substrate in direct contact with each of the graphene nanodisks so that biasing the top gate of the device would cause carrier injection in the lower gate. The injected charge carriers accumulate mainly in the topmost atomic layer,[29] which in this case is the graphene nanodisk array. Both the In−$In_2O_3$ layer and the $BaF_2$ substrate are highly transparent for light wavelengths in the 3−12 $\mu$m range. In comparison with ITO-coated glass, the In−$In_2O_3$ with $BaF_2$ substrate has a higher refractive index that red-shifted the graphene plasmon response but shows lower absorption in the mid-IR, which ensures that the measured absorption is primarily due to the graphene nanodisk array.

The ion-gel layer spin-coated onto the graphene pattern was chemically prepared to yield a high capacitance ($C$ = 2.45 $\mu F/cm^2$) and a low absorption in the mid-infrared range. To prepare the ion gel, 0.56 g of ionic liquid ([EMIM][TFSI]) was first dried under vacuum and then transferred to a glovebox for 4 days; then it was dissolved with 22 mg of PS-PEO-PS (10−44−10 kg $mol^{-1}$) triblock copolymer in 2 mL of dry dichloromethane. The ion-gel layer also serves as a transparent spacer layer between the top Au contact and the bottom layer of graphene nanostructures. The graphene Fermi energy could be effectively tuned from 0.2 to 0.8 eV by applying a top gate bias voltage of 0.2−2.3 V relative to the In−$In_2O_3$ layer lower gate. The Fermi energy is determined through $E_F = \hbar v_F(\pi n)^{1/2}$, where $v_F = 10^6$ m/s is the Fermi velocity, and the carrier density $n$ is calculated by $n = C\Delta V/e$, where $\Delta V$ is the gate bias (referred to as the charge-neutrality point) that was obtained from the $I-V$ characterization measurements. The reflectance ($R$) and transmittance ($T$) of these graphene nanodisk arrays were measured under $N_2$ gas atmosphere using a Fourier transform infrared spectrometer (FTIR, Bruker v80v) coupled to an infrared microscope (36× objective). The absorbance ($A$) is then obtained as $A = 1 - R - T$.

Using a thermal IR source with a large incident illumination spot size (~10 $\mu$m), the FTIR spectra (Figure 2a) exhibit prominent resonances associated with the excitation of plasmons in the graphene disk array. The position and strength of the resonances are very sensitive to the graphene Fermi energy $E_F$. The intrinsic doping from the substrate can be neglected in comparison with the electrostatic doping. As $E_F$ was varied from 0.2 to 0.8 eV, both the reflectance and the absorbance are observed to increase, while the transmittance decreases. The nanostructured graphene sheet boosts the absorbance up to 28% for photon energies around 0.17 eV, while an unpatterned graphene sheet only has ~2.3% absorption at the same optical frequency. Such a drastic enhancement in absorbance is due to the following reasons. First, a carrier density effect is shown: doped graphene opens an optical gap where plasmons can exist without being quenched by coupling to electron−hole pairs (Landau damping), while the number of virtual electron−hole pair transitions allowed is increased, adding to the plasmon strength. Second, a localized surface plasmon resonance (LSPR) effect is demonstrated: a finite nanostructure supports dipolar plasmon resonances that couple directly to incident light. Third, a coupling effect is observed: coherently coupled nanostructures exhibit critical coupling that maximizes absorption with minimum reradiation. This coupling is a far-field effect, as near-field coupling between nanodisks is weak: the peaks in the experimental spectra of nanodisk arrays (Figure 2a) agree very well with the calculated plasmon mode energies for individual nanodisks (Figure 2b) . For example, for $E_F$ = 0.8 eV, the plasmon resonance of an individual nanodisk is 0.18 eV, while for the nanodisk array it shifts to 0.17 eV.

The optical absorption of a perfect graphene nanodisk array can be calculated analytically under the assumption that the disks can be described as dipoles.[28] Using a layer-multiple-scattering method,[30] the reflectance, transmittance, and absorbance were calculated analytically. The results are shown in Figure 2c. The plasmon resonance of an individual graphene disk in the present substrate configuration occurs at an energy

$$\hbar\omega_p \approx (2\alpha\hbar c L_1 E_F/\pi(\varepsilon_1 + \varepsilon_2)D)^{1/2} \quad (1)$$

where $\alpha \sim 1/137$ is the fine-structure constant and $c$ is the speed of light, $L_1$ = 12.5, $\varepsilon_1$ and $\varepsilon_2$ are the permittivities of ion-gel and substrate, respectively, and $D$ is the diameter of the graphene disks.[22]

While the near-field coupling between adjacent nanodisks is very weak, resulting in only very small shifts in the plasmon energies relative to individual nanostructures, the strength and width of the measured spectra show significant deviations from the calculated spectra. The experimental spectra are all systematically broader and have larger areas. A likely factor contributing to this discrepancy is the unavoidable lattice imperfections in the array, which result in strongly inhomogeneously broadened plasmon peaks in the experimental spectra. A close examination of the SEM image in Figure 1b shows that the diameters of the nanodisks range from 50 to 65 nm and the interparticle gap sizes range from 20 to 35 nm. While a detailed analysis of the line shape broadening induced by array


dx.doi.org/10.1021/nl404042h | Nano Lett. 2014, 14, 299−304

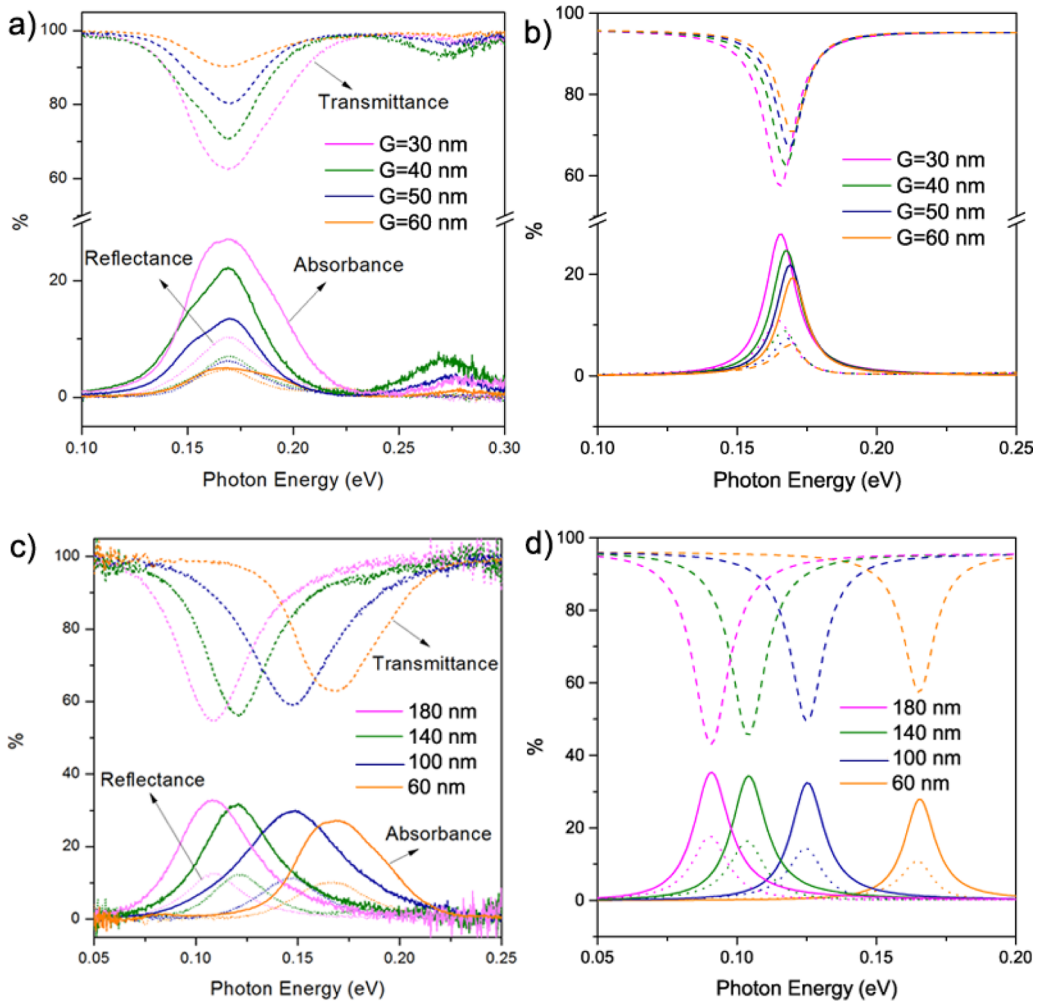


**Figure 3.** (a) FTIR measurements of transmittance, reflectance, and absorbance for 60 nm diameter disks with gap sizes ranging from 30 to 60 nm. (b) Calculated spectra for the same gap sizes. (c) Measured spectra for arrays with 30 nm gap size but disk diameter varying from 60 to 180 nm. (d) Calculated spectra for the structures in panel c. The Fermi energy of the graphene is fixed to $E_F$ = 0.8 eV.

inhomogeneities lies beyond our current computational capabilities, we estimate the contribution of this effect to the line shape by averaging the absorption spectra of a range of disk diameters in an otherwise symmetric lattice. The averaged spectrum, assuming a Gaussian distribution over disk diameters around a central diameter of 60 nm, is shown together with the $E_F$ = 0.8 eV measured data in Figure 2d. The experimentally observed peak broadening is reasonably well reproduced by this approach. The Gaussian averaging was performed for an array period of 90 nm using a weight function $\exp(-(D - D_0/\Delta D)^2)$, with $D_0$ = 60 nm and $\Delta D$ = 10 nm. The graphene phonons (D and G modes) are also located in the mid-infrared region, which may affect the plasmon damping and broaden the resonance line width.[31]

While the near-field coupling between nanodisks is relatively weak, interparticle spacing does have a significant effect on the magnitude of the absorbance, transmittance, and reflectance, via the critical coupling mechanism mentioned above. In Figure 3a we show the measured optical properties of nanodisk arrays with a fixed 60 nm disk diameter, for interdisk gap distances ranging from 30 to 60 nm and $E_F$ = 0.8 eV. The data show that both the reflectance and the absorbance intensities increase with decreasing gap size, while the transmittance decreases. When the gap size is reduced, the coupling increases, giving rise to a slight redshift and strengthening of the absorption peak. The analytical calculations plotted in Figure 3b qualitatively reproduce the experimental results in peak energy and amplitude, but with much narrower peak widths. This discrepancy is likely due to the same inhomogeneous broadening contributions discussed above in connection with Figure 2b. For the smallest gap sizes, the measurements show that the primary absorption peak develops a lower energy shoulder and a weak higher energy feature at nominally 0.27 eV. These features are not reproduced by the analytical calculations but may be caused by hybridized higher energy dipolar or multipolar modes which are absent in our simple model.

The optical properties of graphene nanodisk arrays can also be controlled by varying the disk size. Figure 3c shows the measured optical properties for fixed gap size but disk diameters varying from 60 to 180 nm. The strong redshift of the absorption resonance is primarily due to the increased disk size (see eq 1). The absorption for the largest disks peaks at 32% at 0.1 eV. The calculated spectra shown in Figure 3d are in excellent agreement with the measured data, especially for larger disk diameters, where the nanoscale homogeneities of the nanodisks have less influence.


dx.doi.org/10.1021/nl404042h | Nano Lett. 2014, 14, 299−304

From these studies we can now assess the relative roles of nanodisk size, interdisk spacing, and electrostatic doping in the absorption enhancement of this system. While increasing nanodisk size has a great effect on plasmon tunability, it has a smaller effect on absorption enhancement. Interdisk spacing has the largest effect on absorption enhancement but only minor effects on plasmon tunability. Electrostatic doping of the arrays, due to an applied voltage, affects both the plasmon energies and the enhanced absorption (and transmittance and reflectance) of the arrays in a coupled manner.

While the enhanced absorption we observe here is quite large, because the device geometry lacks an underlying mirror plane it should not be compared directly with the graphene perfect absorber (100% level) proposed in an earlier publication.[28,32] The maximum absorption predicted for an array placed in a symmetric dielectric environment is 50%, so that our observation of 30% absorption in this structure is still a remarkably high result. More careful matching of the dielectric environment above and below the graphene nanodisk array, and more precise fabrication to reduce the effects of inhomogeneous broadening on the peak lineshapes, are both likely to bring the maximum absorption closer to this theoretically predicted value. An additional factor of 2 (i.e., 60%) should be readily obtained in reflection by placing a nanodisk array on a metallic reflecting plane, where the incident light makes two passes (forward and reflected) through the graphene array, doubling the absorbance enhancement when the two waves are in phase.

In conclusion, we have experimentally demonstrated that, with a closely packed array of single-atomic-layer graphene nanodisks, the optical absorption of graphene can be increased to above 30% at resonance frequencies in the infrared, a value substantially larger than the 2.3% absorption exhibited by a single undoped graphene monolayer. The relative dependence of this effect on nanodisk size, interparticle spacing, and voltage-driven electrostatic doping, has been determined. These results point to a promising future for graphene as an adaptive plasmonic material with properties that may give rise to electro-optic devices across the infrared region of the spectrum.

## AUTHOR INFORMATION


### Corresponding Authors

*E-mail: zhyfang@pku.edu.cn.
*E-mail: halas@rice.edu.


### Notes

The authors declare no competing financial interest.

## ACKNOWLEDGMENTS

The work is supported by National Natural Science Foundation of China (grant no. 11374023; 61176120) and the National Basic Research Program of China (973 Program), grant nos. 2007CB936800 and 2012CB933004l. N.J.H. and P.N. acknowledge support from the Robert A. Welch Foundation under grants C-1220 and C-1222, the Office of Naval Research under grant N00014-10-1-0989, and the DoD NSSEFF (N00244-09-1-0067). F.J.G.deA. acknowledges support from the Spanish MEC (MAT2010-14885). Z.L. and P.M.A. acknowledge funding support from the U.S. Office of Naval Research MURI grant N000014-09-1-1066.

## REFERENCES


(1) Bonaccorso, F.; Sun, Z.; Hasan, T.; Ferrari, A. C. Graphene photonics and optoelectronics. *Nat. Photonics* **2010**, *4*, 611−622.

(2) Ju, L.; Geng, B. S.; Horng, J.; Girit, C.; Martin, M.; Hao, Z.; Bechtel, H. A.; Liang, X. G.; Zettl, A.; Shen, Y. R.; Wang, F. Graphene plasmonics for tunable terahertz metamaterials. *Nat. Nanotechnol.* **2011**, *6*, 630−634.

(3) Liu, M.; Yin, X. B.; Ulin-Avila, E.; Geng, B. S.; Zentgraf, T.; Ju, L.; Wang, F.; Zhang, X. A graphene-based broadband optical modulator. *Nature* **2011**, *474*, 64−67.

(4) Novoselov, K. S.; Geim, A. K.; Morozov, S. V.; Jiang, D.; Katsnelson, M. I.; Grigorieva, I. V.; Dubonos, S. V.; Firsov, A. A. Two-dimensional gas of massless Dirac fermions in graphene. *Nature* **2005**, *438*, 197−200.

(5) Novoselov, K. S.; Geim, A. K.; Morozov, S. V.; Jiang, D.; Zhang, Y.; Dubonos, S. V.; Grigorieva, I. V.; Firsov, A. A. Electric field effect in atomically thin carbon films. *Science* **2004**, *306*, 666−669.

(6) Wang, X.; Zhi, L. J.; Mullen, K. Transparent, conductive graphene electrodes for dye-sensitized solar cells. *Nano Lett.* **2008**, *8*, 323−327.

(7) Williams, G.; Seger, B.; Kamat, P. V. $TiO_2$-graphene nanocomposites. UV-assisted photocatalytic reduction of graphene oxide. *ACS Nano* **2008**, *2*, 1487−1491.

(8) Xia, F. N.; Mueller, T.; Lin, Y. M.; Valdes-Garcia, A.; Avouris, P. Ultrafast graphene photodetector. *Nat. Nanotechnol.* **2009**, *4*, 839−843.

(9) Zhang, H.; Lv, X. J.; Li, Y. M.; Wang, Y.; Li, J. H. P25-Graphene Composite as a High Performance Photocatalyst. *ACS Nano* **2010**, *4*, 380−386.

(10) Zhang, Y. B.; Tang, T. T.; Girit, C.; Hao, Z.; Martin, M. C.; Zettl, A.; Crommie, M. F.; Shen, Y. R.; Wang, F. Direct observation of a widely tunable bandgap in bilayer graphene. *Nature* **2009**, *459*, 820−823.

(11) Mak, K. F.; Sfeir, M. Y.; Wu, Y.; Lui, C. H.; Misewich, J. A.; Heinz, T. F. Measurement of the Optical Conductivity of Graphene. *Phys. Rev. Lett.* **2008**, *101*, 196405.

(12) Pirruccio, G.; Moreno, L. M.; Lozano, G.; Rivas, J. G. Coherent and Broadband Enhanced Optical Absorption in Graphene. *ACS Nano* **2013**, *7*, 4810−4817.

(13) Naik, G. V.; Shalaev, V. M.; Boltasseva, A. Alternative Plasmonic Materials: Beyond Gold and Silver. *Adv. Mater.* **2013**, *25*, 3264−3294.

(14) Echtermeyer, T. J.; Britnell, L.; Jasnos, P. K.; Lombardo, A.; Gorbachev, R. V.; Grigorenko, A. N.; Geim, A. K.; Ferrari, A. C.; Novoselov, K. S. Strong plasmonic enhancement of photovoltage in graphene. *Nat. Commun.* **2011**, *2*, 458.

(15) Fang, Z. Y.; Liu, Z.; Wang, Y. M.; Ajayan, P. M.; Nordlander, P.; Halas, N. J. Graphene-Antenna Sandwich Photodetector. *Nano Lett.* **2012**, *12*, 3808−3813.

(16) Fang, Z. Y.; Wang, Y. M.; Liu, Z.; Schlather, A.; Ajayan, P. M.; Koppens, F. H. L.; Nordlander, P.; Halas, N. J. Plasmon-Induced Doping of Graphene. *ACS Nano* **2012**, *6*, 10222−10228.

(17) Emani, N. K.; Chung, T. F.; Ni, X. J.; Kildishev, A. V.; Chen, Y. P.; Boltasseva, A. Electrically Tunable Damping of Plasmonic Resonances with Graphene. *Nano Lett.* **2012**, *12*, 5202−5206.

(18) Grigorenko, A. N.; Polini, M.; Novoselov, K. S. Graphene plasmonics. *Nat. Photonics* **2012**, *6*, 749−758.

(19) Jablan, M.; Buljan, H.; Soljacic, M. Plasmonics in graphene at infrared frequencies. *Phys. Rev. B* **2009**, *80*, 245435.

(20) Koppens, F. H. L.; Chang, D. E.; de Abajo, F. J. G. Graphene Plasmonics: A Platform for Strong Light-Matter Interactions. *Nano Lett.* **2011**, *11*, 3370−3377.

(21) Brar, V. W.; Jang, M. S.; Sherrott, M.; Lopez, J. J.; Atwater, H. A. Highly Confined Tunable Mid-Infrared Plasmonics in Graphene Nanoresonators. *Nano Lett.* **2013**, *13*, 2541−2547.

(22) Fang, Z. Y.; Thongrattanasiri, S.; Schlather, A.; Liu, Z.; Ma, L. L.; Wang, Y. M.; Ajayan, P. M.; Nordlander, P.; Halas, N. J.; de Abajo, F. J. G. Gated Tunability and Hybridization of Localized Plasmons in Nanostructured Graphene. *ACS Nano* **2013**, *7*, 2388−2395.

(23) Dean, C. R.; Young, A. F.; Meric, I.; Lee, C.; Wang, L.; Sorgenfrei, S.; Watanabe, K.; Taniguchi, T.; Kim, P.; Shepard, K. L.;

Hone, J. Boron nitride substrates for high-quality graphene electronics. *Nat. Nanotechnol.* **2010**, *5*, 722−726.
(24) Yan, H. G.; Li, X. S.; Chandra, B.; Tulevski, G.; Wu, Y. Q.; Freitag, M.; Zhu, W. J.; Avouris, P.; Xia, F. N. Tunable infrared plasmonic devices using graphene/insulator stacks. *Nat. Nanotechnol.* **2012**, *7*, 330−334.
(25) Chen, C. F.; Park, C. H.; Boudouris, B. W.; Horng, J.; Geng, B. S.; Girit, C.; Zettl, A.; Crommie, M. F.; Segalman, R. A.; Louie, S. G.; Wang, F. Controlling inelastic light scattering quantum pathways in graphene. *Nature* **2011**, *471*, 617−620.
(26) Hwang, E. H.; Das Sarma, S. Dielectric function, screening, and plasmons in two-dimensional graphene. *Phys. Rev. B* **2007**, *75*, 205418.
(27) Polini, M.; Asgari, R.; Borghi, G.; Barlas, Y.; Pereg-Barnea, T.; MacDonald, A. H. Plasmons and the spectral function of graphene. *Phys. Rev. B* **2008**, *77*, 081411.
(28) Thongrattanasiri, S.; Koppens, F. H. L.; de Abajo, F. J. G. Complete Optical Absorption in Periodically Patterned Graphene. *Phys. Rev. Lett.* **2012**, *108*, 047401.
(29) Lang, N. D.; Kohn, W. Theory of Metal Surfaces - Charge Density and Surface Energy. *Phys. Rev. B* **1970**, *1*, 4555.
(30) Stefanou, N.; Yannopapas, V.; Modinos, A. Heterostructures of photonic crystals: frequency bands and transmission coefficients. *Comput. Phys. Commun.* **1998**, *113*, 49−77.
(31) Yan, H. G.; Low, T.; Zhu, W. J.; Wu, Y. Q.; Freitag, M.; Li, X. S.; Guinea, F.; Avouris, P.; Xia, F. N. Damping pathways of mid-infrared plasmons in graphene nanostructures. *Nat. Photonics* **2013**, *7*, 394−399.
(32) Engheta, N. In *Digest of the 2002 IEEE AP-S International Symposium*, San Antonio, TX; IEEE: New York, 2002; Vol. 2, pp 392−395.